

## Using Density Functional Theory To Design DNA Base Analogues with Low Oxidation Potentials

Mu-Hyun Baik,<sup>†</sup> Joel S. Silverman,<sup>†</sup> Ivana V. Yang,<sup>†</sup> Patricia A. Ropp,<sup>†</sup> Veronika A. Szalai,<sup>†</sup> Weitao Yang,<sup>‡</sup> and H. Holden Thorp<sup>\*,†</sup>

Department of Chemistry, University of North Carolina at Chapel Hill, Chapel Hill, North Carolina 27599-3290, and Department of Chemistry, Duke University, Durham, North Carolina 27708

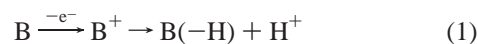
Received: February 18, 2001; In Final Form: April 30, 2001

The oxidizability of substituted nucleobases was evaluated through theoretical calculations and the ability of individual bases to induce current enhancement in the cyclic voltammograms of metal complexes. Formation of the guanine derivatives 7-deazaguanine and 8-oxoguanine is known to lower the energy for oxidation of guanine. The similar derivatives of adenine were examined and gave lower predicted redox energies as well as current enhancement with Ru(bpy)<sub>3</sub><sup>2+</sup> (7-deazaadenine) and Fe(bpy)<sub>3</sub><sup>2+</sup> (8-oxoadenine). Oxidizable, substituted pyrimidines were identified using a computational library that gave 5-aminocytosine and 5-aminouracil as promising electron donors. Again, these predictions were verified using catalytic electrochemistry. In addition, the computations predicted that 6-aminocytosine would be redox-active but not as easily oxidized as 5-aminocytosine, which was also confirmed experimentally. In addition to calculating the relative one-electron redox potentials, we used calculations to evaluate the loss of a proton that occurs from the initially formed radical cation. These calculations gave results consistent with the experiments, and in the case of 8-oxoadenine, the relative redox reactivity could be predicted only when the proton loss step was considered. These substituted bases constitute building blocks for highly redox-active nucleic acids, and the associated theoretical model provides powerful predictability for designing new redox-active nucleobases.

The redox activity of DNA is under intense examination as a platform for developing miniaturized devices<sup>1–3</sup> and for designing biological assays.<sup>4–7</sup> Since the redox potential of guanine is much lower than that of the other bases, guanine often acts as a low-energy bridge for achieving strong electronic coupling along the DNA axis,<sup>8–11</sup> a convenient donor for monitoring remote electron transfer,<sup>12,13</sup> or a redox-active moiety for electrochemical analysis.<sup>4–6</sup> The utility of DNA redox chemistry would be considerably expanded by the availability of additional nucleobases that are easily oxidized and mimic the structure of duplex DNA. For example, greater electronic coupling along the DNA axis could be obtained with a higher population of redox-active bases,<sup>14,15</sup> and additional electrochemical assays could be envisioned if the limitation of using only guanine as the electron donor were removed.<sup>4–6</sup>

We report here on a set of oxidizable DNA bases that are minimally substituted compared to the native parents and were identified on the basis of density functional theory (DFT)<sup>16,17</sup> calculations self-consistently coupled to the conductor-like solvation model (COSMO).<sup>18,19</sup> The continuum solvation model has been used successfully to predict solution redox potentials in the literature.<sup>20–33</sup> The case of oxidation of nucleobases, particularly guanine, has been examined extensively by similar calculations.<sup>34,35</sup> In our case, we wished not only to model the simple one-electron oxidation but also to include the effect of deprotonation of the one-electron oxidation product, which gives a strong pH dependence of the redox potentials.<sup>36–39</sup> We have shown recently that ground-state oxidation of guanine by Ru-

(bpy)<sub>3</sub><sup>3+</sup> (bpy = 2,2'-bipyridine) proceeds via a proton-coupled electron transfer,<sup>40</sup> which has been incorporated into our computational model. The model therefore aims to predict the standard redox potentials  $E^\circ$  of the proton-coupled redox processes for the overall reaction



The value for  $E_{1/2}$  determined in electrochemical measurements is dependent on the concentration of the different deprotonated and oxidized products present at the given pH.<sup>41</sup> A theoretical evaluation of such a dynamic process must include a survey of the energetics of all accessible species; however, we were able to simplify our model by considering only the first deprotonation product of the cationic nucleobase radical. Our goals of identifying features dictating the oxidation potentials and deducing a rational strategy for tuning the oxidation potential could be achieved by concentrating only on the first step. The calculated and experimentally observed redox potentials could then be rationalized on the basis of the electronic structure calculations.

While there are a number of purines with oxidation potentials that can be accessed in a room-temperature, neutral solution,<sup>36,42,43</sup> identifying pyrimidines with accessible redox potentials is a more challenging task. There is only one report of redox activity from pyrimidines (5-hydroxyuridine and 5-hydroxycytosine),<sup>44</sup> and these were examined in multicomponent systems where multiple electron transfers are possible. Redox-active pyrimidines have been more elusive because to reach the potential of guanine requires a drop in redox energy of ~1 eV based on estimates of cytosine and thymine potentials.<sup>42</sup> An

<sup>†</sup> University of North Carolina.

<sup>‡</sup> Duke University.

**TABLE 1: Gas-Phase Oxidation Potentials (in eV) Evaluated Using Enthalpy Only ( $\Delta H$ ) and Corrected for Zero-Point Energy and Entropy ( $\Delta G$ )<sup>a</sup>**

	$\Delta H$	$\Delta G$	exptl <sup>b</sup>
guanine	7.676 (-2.2)	7.667 (-2.4)	7.77
adenine	8.086 (-4.0)	8.075 (-4.3)	8.26
cytosine	8.564 (-2.7)	8.532 (-3.4)	8.68
thymine	8.708 (-3.7)	8.682 (-4.3)	8.87
xanthine	8.438 (-2.6)	8.430 (-2.8)	8.55
isocytosine	8.434 (-0.1)	8.401 (-0.9)	8.44
hypoxanthine	8.430 (-0.2)	8.395 (-1.0)	8.44
6-methylcytosine	8.261 (-2.7)	8.192 (-4.3)	8.38
5-aminocytosine	7.530	7.527	
5-aminouracil	7.669	7.694	
6-aminocytosine	7.885	7.869	
8-oxoguanine	7.389	7.409	
8-oxoadenine	7.974	7.973	
8-bromoguanine	7.603	7.604	
7-deazaguanine	7.211	7.218	
7-deazaadenine	7.599	7.632	

<sup>a</sup> Differences between experimental and theoretical potentials are given in parentheses (kilocalories per mole). <sup>b</sup> Experimental values taken from ref 64.

additional experimental complication is that fewer simply substituted pyrimidine analogues are readily available. We therefore generated a computational library containing native pyrimidines modified with no more than one functional group, where only the sites not directly involved in DNA base pairing were considered for modification. The functional moieties sampled in the computational library included chloro, fluoro, bromo, amino, methyl, hydroxyl, carboxylic, and methoxy groups. Substitutions of a ring carbon with nitrogen to generate the deaza analogue of the base were also included. The most promising candidates from the computational library were synthesized and evaluated for oxidation by metal mediators.

## Experimental Section

**Computational Details.** We have used the Amsterdam density functional package (ADF)<sup>45</sup> to carry out all calculations. A triple- $\zeta$  STO basis set was utilized with one set of polarization functions as provided in the package (basis set IV, comparable to 6-311G\*), together with the VWN local exchange-correlation potential,<sup>46</sup> augmented by exchange and correlation functionals as suggested by Perdew and Wang (PW91).<sup>47</sup> The 1s orbitals of the atoms carbon, nitrogen, and oxygen were treated by the frozen core approximation. Solvation effects have been included using the conductor-like screening model (COSMO) suggested by Klamt and Schüürmann<sup>18</sup> and implemented in ADF by Pye and Ziegler.<sup>19</sup> The crucial part of the solvation calculation is the choice of the radii that define the cavity representing the

solute. The solvent-excluding surface was chosen and was constructed using the following radii: H, 1.16 Å; C, 2.30 Å; N, 1.40 Å; O, 1.40 Å; and Br, 2.40 Å. A dielectric constant of 78.4 was used for water. All geometries have been fully optimized using the gradient-corrected functionals without any symmetry constraints. With the optimized gas-phase structure as a starting point, the solution geometries were obtained by a new full geometry optimization with the COSMO potential applied. Vibrational frequency calculations were carried out using the double-differentiation method in a finite difference scheme. Both gas-phase and solution frequencies have been computed and used to derive the zero-point energies and entropic corrections for the gas-phase and solution enthalpies, respectively. We have applied the spin-unrestricted formalism to all calculations.

**Experiments.** [Os(bpy)<sub>3</sub>]Cl<sub>2</sub>, [Ru(bpy)<sub>3</sub>]Cl<sub>2</sub>, [Fe(bpy)<sub>3</sub>]Cl<sub>2</sub>, 7-deazaguanosine triphosphate, 7-deazaadenosine triphosphate, and 8-bromoguanosine monophosphate were purchased from Sigma-Aldrich and used without further purification. 5-Aminodeoxycytidine and 6-aminodeoxycytidine were synthesized according to a published procedure,<sup>48</sup> as was 5-aminodeoxyuridine.<sup>49</sup> Cyclic voltammograms were collected using a BAS100B electrochemical analyzer with a single-compartment voltammetric cell equipped with an indium tin oxide (ITO) working electrode, a Pt-wire counter electrode, and an Ag/AgCl reference electrode. The ITO electrodes were purchased from Delta Technologies, Inc. The Ag/AgCl electrode was purchased from Cypress, Inc. For solutions containing Os(bpy)<sub>3</sub><sup>2+</sup>, cyclic voltammograms from 0 to 0.8 V were taken at a scan rate of 25 mV/s. For solutions containing Ru(bpy)<sub>3</sub><sup>2+</sup>, cyclic voltammograms from 0 to 1.3 V were taken at a scan rate of 25 mV/s. Background scans of buffer alone were collected and subtracted from scans of metal complexes alone and with nucleobases.

## Results

**Computational Library and Experimental Evaluation.** In previous studies from our laboratory, the one-electron oxidation of guanine has been monitored via an enhancement in the oxidative current in the cyclic voltammogram (CV) of Ru(bpy)<sub>3</sub><sup>2+</sup>,<sup>50–52</sup> which is oxidized to the 3+ form at a potential similar to that of guanine (~1.29 V, all potentials relative to the SHE). Oxidation of the remaining nucleobases cannot be observed in this manner since the redox potentials for adenine, thymine, and cytosine are much less accessible to Ru(bpy)<sub>3</sub><sup>3+</sup>. We<sup>53,54</sup> and others<sup>38,44,55,56</sup> have observed that the guanine derivatives 8-oxoguanine and 7-deazaguanine exhibit lower redox potentials than guanine, and these bases are accordingly oxidized by Os(bpy)<sub>3</sub><sup>3+</sup> ( $E_{1/2} = 0.84$  V)<sup>53</sup> and Fe(bpy)<sub>3</sub><sup>3+</sup>

**TABLE 2: Solution Oxidation Potentials (in eV) Evaluated Using Enthalpy Only ( $\Delta H$ ) and Corrected for Zero-Point Energy and Entropy ( $\Delta G$ )**

	$\Delta H(\text{calcd})$	$\Delta G(\text{calcd})$	$\Delta\Delta G(\text{calcd})$	$\Delta\Delta E^{1/2}(\text{calcd})$	$E^{1/2}(\text{exptl})$
guanine	5.738	5.748	0	0	1.29 <sup>a</sup>
adenine	6.098	6.091	0.343	0.13	1.42 <sup>b</sup>
cytosine	6.504	6.527	0.779	0.31	1.60 <sup>b</sup>
thymine	6.582	6.562	0.814	0.41	1.70 <sup>b</sup>
5-aminocytosine	5.156	5.208	-0.540	-0.54	~0.75 <sup>c</sup>
5-aminouracil	5.304	5.312	-0.436	-0.54	~0.75 <sup>c</sup>
6-aminocytosine	5.705	5.750	0.002	0.00	~1.30 <sup>c</sup>
8-oxoguanine	5.388	5.461	-0.287	-0.55	0.74 <sup>a</sup>
8-oxoadenine	5.775	5.817	0.069	-0.37	0.92 <sup>b</sup>
8-bromoguanine	5.733	5.788	0.040	0.01	~1.30 <sup>c</sup>
7-deazaguanine	5.312	5.344	-0.404	-0.32	~0.97 <sup>c</sup>
7-deazaadenine	5.649	5.675	-0.073	0.01	~1.30 <sup>c</sup>

<sup>a</sup> From refs 36 and 38. <sup>b</sup> From refs 11 and 42. <sup>c</sup> From this work.

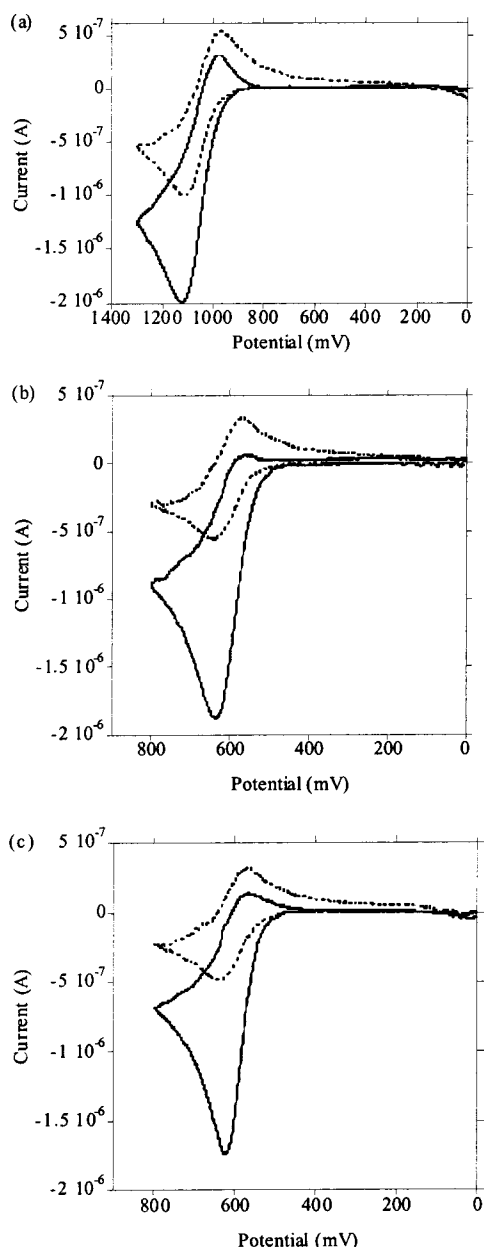


**Figure 1.** Cyclic voltammograms of  $\text{Ru}(\text{bpy})_3^{2+}$  and  $\text{Os}(\text{bpy})_3^{2+}$  with modified nucleosides recorded at a scan rate of 25 mV/s in 50 mM sodium phosphate (pH 7.0) with 780 mM NaCl. (a) Voltammograms of 50  $\mu\text{M}$   $\text{Ru}(\text{bpy})_3^{2+}$  alone (---) or in the presence of 12.5  $\mu\text{M}$  8-bromoguanosine monophosphate (—). (b) Voltammograms of 25  $\mu\text{M}$   $\text{Os}(\text{bpy})_3^{2+}$  alone (---) or in the presence of 25  $\mu\text{M}$  5-aminodeoxycytidine (—). (c) Voltammograms of 25  $\mu\text{M}$   $\text{Os}(\text{bpy})_3^{2+}$  alone (---) or in the presence of 25  $\mu\text{M}$  5-aminodeoxyuridine (—).

( $E_{1/2} = 1.07$  V),<sup>54</sup> respectively. We therefore reasoned that the same analogues of adenine should exhibit lower redox potentials than native adenine and might in fact be as or more easily oxidized than guanine. Indeed, 7-deazaadenine shows significant current enhancement with  $\text{Ru}(\text{bpy})_3^{3+}$ , and 8-oxoadenine is reactive with  $\text{Fe}(\text{bpy})_3^{3+}$  (data given in Supporting Information),<sup>57</sup> giving the same trend in reactivity as the analogous guanine derivatives. Reactivity of 8-oxoadenine in a multicomponent redox system has been observed previously.<sup>44</sup>

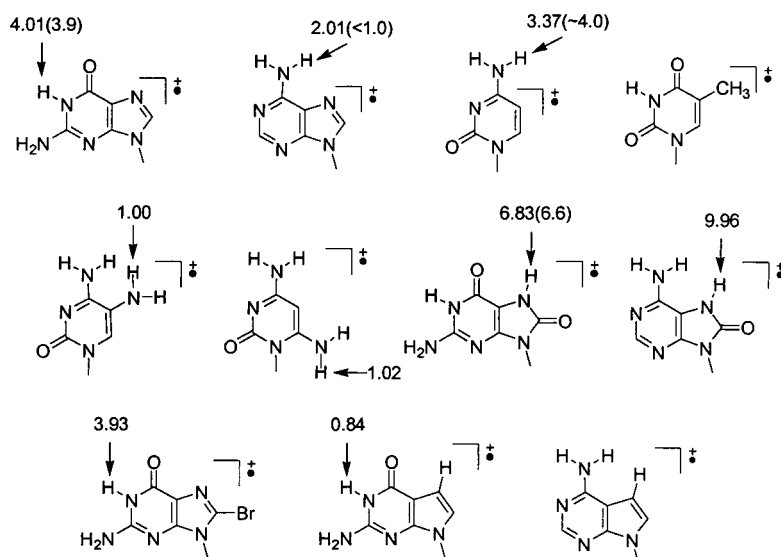
To verify that the computations gave the right trends, we also included in our study the 8-oxo and 7-deaza derivatives of adenine and guanine as well as 8-bromoguanine, which served as a negative control (see below). These compounds were evaluated with computational methods based on density func-

tional theory (DFT)<sup>16,17</sup> self-consistently combined with the conductor-like solvation model (COSMO)<sup>18,19</sup> to compute solution-phase energies of oxidation. In our computational model, we use the nucleobase without the sugar and the phosphate groups. The experimental evaluation, however, was conducted using the nucleotides. We have explored the electronic influence of the sugar-phosphate moiety on the purine ring and found a very minor effect of the ribose moiety on the oxidation potentials, which is in good agreement with observations reported recently by Guerra et al.<sup>58–60</sup>

The computed gas-phase and solution oxidation potentials of the most interesting nucleobases in our library are summarized in Tables 1 and 2, respectively. The enthalpic energy differences based on the optimized geometries,  $\Delta H$ , were evaluated initially without accounting for the zero-point energy (ZPE) and entropic corrections. The corrected free energy changes,  $\Delta G$ , are also listed, allowing us to compare the enthalpic and entropic contributions to the oxidation potential. Among the natural nucleobases, the lowest oxidation potential in solution was for guanine (5.74 eV). Adenine is more difficult to oxidize with a potential of 6.10 eV. The oxidation potentials of the pyrimidine bases are roughly 0.5 eV higher than that of adenine. The  $\Delta H$ -based estimates reproduce the expected shift to lower potentials for 8-oxoguanine, 7-deazaguanine, and 7-deazaadenine. Only the computed potential of 8-oxoadenine, which was expected to be significantly lower than that of guanine according to experimental data given here and elsewhere,<sup>44</sup> is too high; both  $\Delta H$ - and  $\Delta G$ -based potentials are  $\sim 0.3$  eV higher than that of guanine. We have explored possible flaws in the computational model, such as the existence of different tautomers<sup>61–63</sup> of 8-oxoadenine that might give access to a lower oxidation potential, and concluded that the oxidation potential of 8-oxoadenine cannot be compared to those of the other systems of the series without including the proton loss step (see below).

Initially, we expected the oxidation potential of 8-bromoguanine to be higher than that of guanine due to the electron-withdrawing properties of bromine. However, the positive reaction with  $\text{Ru}(\text{bpy})_3^{3+}$  (Figure 1a) suggests a redox potential for 8-bromoguanine that is similar to that of guanine, which was also predicted correctly by the computational model. The calculations show that the lack of an effect of the bromine substituent is due to the poor overlap of the Br 4p orbital with the ring  $\pi$  system.

The computational library produced 5-aminocytosine, 5-aminouracil, and 6-aminocytosine as likely oxidizable pyrimidines. The COSMO calculations suggest an oxidation potential of 5.156 eV (0.72 V vs the SHE<sup>64</sup>) for 5-aminocytosine which is 0.58 eV lower than that of guanine and even lower than that of 8-oxoguanine (Table 2). A similar shift is predicted for 5-aminouracil. It is not surprising that attaching a strong  $\pi$  donor, such as an amino group, decreases the oxidation potential since the highest occupied molecular orbital (HOMO) becomes more electron rich. However, the magnitude of the shift observed upon addition of the amino group at the 5-position is remarkable. Since 5-aminocytosine and 5-aminouracil bases gave much lower predicted redox energies than guanine, we expected these compounds to react with low-potential mediators. Indeed, both of these compounds gave large current enhancements with  $\text{Os}(\text{bpy})_3^{2+}$  (Figure 1b,c). Substitution of an amino group at the 6-position of cytosine resulted in a significant shift of the oxidation potential as well. The predicted redox potential for 6-aminocytosine was similar to that of guanine, and current enhancement was accordingly observed for  $\text{Ru}(\text{bpy})_3^{2+}$  but not  $\text{Os}(\text{bpy})_3^{2+}$  (data given in Supporting Information).

TABLE 3: Computed  $pK_a$  Values of the Cationic Radicals<sup>a</sup>

	$pK_a(\text{calcd})$	$pK_a(\text{exptl})$	$\Delta G^H$	$\Delta\Delta G^H$ <sup>b</sup>	$E^\circ(\text{calcd})$	$E^\circ(\text{exptl})$	$E^{1/2}(\text{exptl})$
guanine	4.01	3.9 <sup>c</sup>	6.108	0.360	1.67	1.58	1.29 <sup>c</sup>
adenine	2.01	< 1.0 <sup>c</sup>	6.568	0.477	2.14	2.03	1.42 <sup>d</sup>
cytosine	3.37	~4.0 <sup>c</sup>	6.932	0.405	2.50	2.53	1.60 <sup>d</sup>
thymine	6.40	3.6 <sup>c</sup>	6.765	0.203	2.34	2.63	1.70 <sup>d</sup>
5-aminocytosine	1.00		5.752	0.544	1.32		~0.75 <sup>e</sup>
5-aminouracil	2.06		5.794	0.482	1.36		~0.75 <sup>e</sup>
6-aminocytosine	1.02		6.293	0.543	1.86		~1.30 <sup>e</sup>
8-oxoguanine	6.83	6.6 <sup>c</sup>	5.660	0.199	1.23		0.74 <sup>c</sup>
8-oxoadenine	9.96		5.831	0.014	1.60		0.92 <sup>d</sup>
8-bromoguanine	3.93		6.159	0.371	1.73		~1.30 <sup>e</sup>
7-deazaguanine	0.84		5.898	0.554	1.47		~0.97 <sup>e</sup>
7-deazaadenine	-1.46		6.365	0.690	1.93		~1.30 <sup>e</sup>

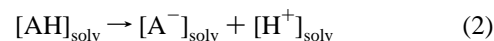
<sup>a</sup> Available experimental values are given in parentheses. <sup>b</sup>  $\Delta\Delta G^H$  is the energy difference between the redox reaction, including the deprotonation ( $\Delta G^H$ ), and that considering the electron removal only ( $\Delta G$  in Table 2). <sup>c</sup> From refs 36 and 38. <sup>d</sup> From refs 11 and 42. <sup>e</sup> From this work.

**Gas-Phase Calculations.** Steenken and co-workers have provided highly reliable data for the oxidation in solution of adenosine, guanosine, and 8-oxoguanosine,<sup>37,38</sup> but data of similar quality are difficult to obtain for the other nucleosides due to the high potentials that are involved. However, accurate gas-phase oxidation potentials can be obtained through mass spectrometry.<sup>65</sup> To assess the level of reliability of our computational model, we have carried out gas-phase calculations on a number of nucleobases in the same theoretical framework that will be used in the solvated models and that can be compared to the known gas-phase potentials (Table 1).

Gas-phase oxidation potentials of the natural nucleobases have previously been calculated using *ab initio* methods by Saito and co-workers<sup>35</sup> and Houk and co-workers.<sup>34</sup> Our results given in Table 1 are in good agreement with these reports and the experimental values. The ZPE and entropy corrections have a minor effect on the oxidation potential, which is not surprising since the extended  $\pi$  system of the bases will allow an efficient distribution of the positive charge, causing relatively small changes in the force constants between the neutral and cationic forms of the base. The differences of the calculated and experimental oxidation potentials are given in parentheses (in kilocalories per mole) and are in all cases less than 5 kcal/mol. We note that the computed values are systematically lower than the experimental potentials.

**Proton Loss.** To construct a more complete model of nucleobase oxidation, the proton loss step must be included, since we have observed that on the time scale of the electrocatalytic reaction, proton loss partly governs the oxidation rate.<sup>40</sup>

Therefore, an evaluation of the acidity of the one-electron oxidation product was undertaken initially. Absolute  $pK_a$  values can be computed by calculating the free energy change for the reaction



$$\Delta G^{\text{deprot}} = -\Delta G(\text{AH}) + \Delta G(\text{A}^-) + \Delta G(\text{H}^+) \quad (3)$$

where  $\Delta G(\text{AH})$  and  $\Delta G(\text{A}^-)$  are the ZPE and entropy-corrected free energies of the protonated and deprotonated forms of the nucleobase in solution, respectively. The free energy of the proton,  $\Delta G(\text{H}^+)$ , cannot be computed simply using the continuum model, since the formation of  $\text{H}_3\text{O}^+$  and its explicit interaction with water have to be accounted for to obtain a physically reasonable energy. Following the procedure commonly used in the literature,<sup>66-69</sup> we compute  $\Delta G(\text{H}^+)$  as

$$\Delta G(\text{H}^+) = \Delta H^{\text{vac}}(\text{H} \rightarrow \text{H}^+) + T\Delta S + \frac{5}{2}RT + \Delta G^{\text{solv}}(\text{H}^+) \quad (4)$$

where  $\Delta H^{\text{vac}}$  is the gas-phase ionization potential of hydrogen,  $T = 298.15$  K,  $S$  is the translational entropy of a free hydrogen atom (26.04 eu) calculated using the Sackur-Tetrode equation,  $R$  is the universal gas constant, and  $\Delta G^{\text{solv}}$  is the solvation free energy of a proton (-262.23 kcal/mol).<sup>70</sup> At room temperature, eq 4 gives a  $\Delta G(\text{H}^+)$  of 12.37 kcal/mol, which is the energy to be added to the calculated energy differences of the protonated and deprotonated forms of the nucleobases. The equilibrium

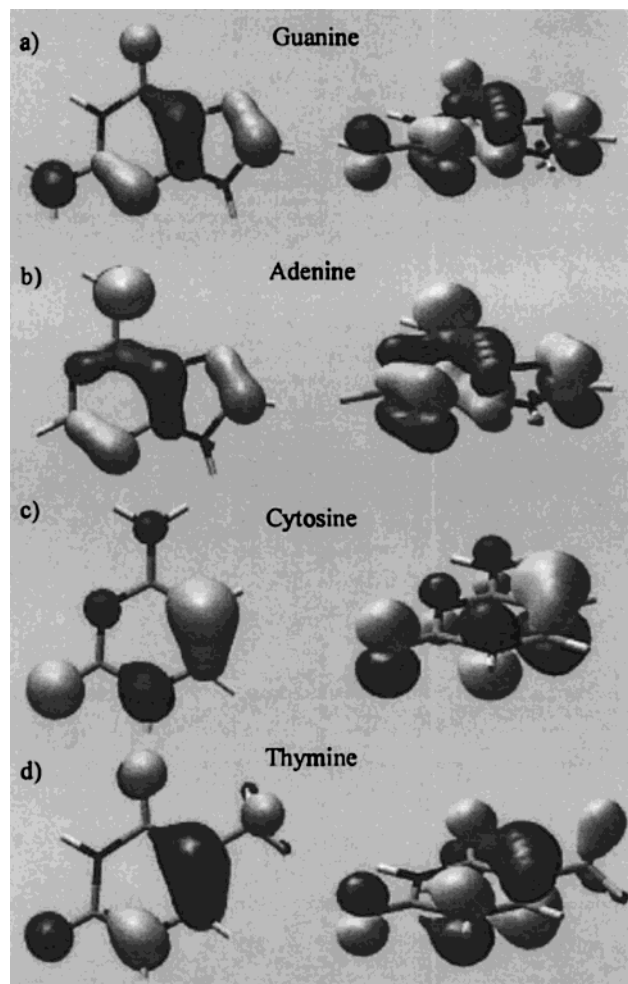


**Figure 2.** Three-dimensional plots of the HOMO of all four nucleobases. Two views of the same orbital are shown.

constant  $K_a$  of the deprotonation reaction (eq 2) and the corresponding  $pK_a$  value of the nucleobase can be computed using

$$\Delta G^{\text{deprot}} = -RT \ln(K_a) \quad (5)$$

$$pK_a = \frac{\Delta G^{\text{deprot}}}{2.303RT} = \frac{\Delta G^{\text{deprot}} (\text{in kcal/mol})}{1.3658} \quad (6)$$

The entropic corrections and ZPE in solution have been derived from vibrational frequency calculations computed using the COSMO correction; the only significant entropy contribution is the vibrational entropy. By recomputing the cavity shape and COSMO charge distribution for each of the displaced geometries in the finite difference runs, our model assumes a perfectly flexible solute cavity that follows the vibrational modes without delays. The energy components of all nucleobases used in this study are given in the Supporting Information. (Note that the deprotonation reaction given in eq 2 is naturally an endothermic process for all acids with positive  $pK_a$  values.) Since the  $pK_a$  values of the cationic nucleobase radicals are typically positive, the standard redox potential  $E^\circ$  ( $=\Delta G - 4.43$  eV) of each base is expected to become more positive compared to the values listed in Table 2.

The free energies of oxidation that account for the deprotonation and the computed  $pK_a$  values are listed in Table 3 as  $\Delta G^H$ . The correction to  $\Delta G$ , the reaction energy only considering the electron detachment (Table 2), is listed as  $\Delta\Delta G^H$  in Table

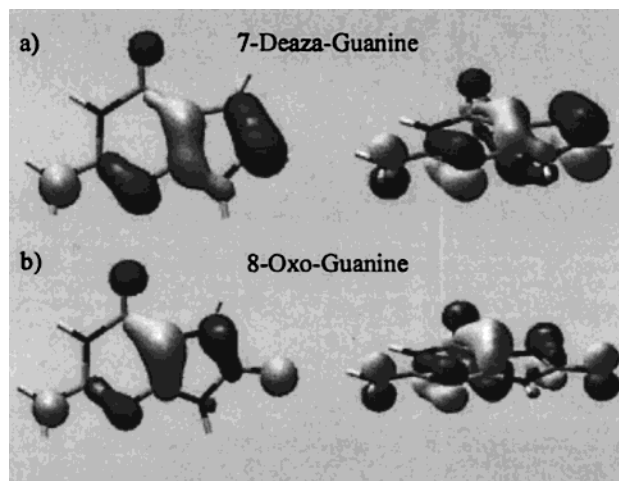


**Figure 3.** Three-dimensional plots of the HOMO of 7-deazaguanine and 8-oxoguanine. Two views of the same orbital are shown.

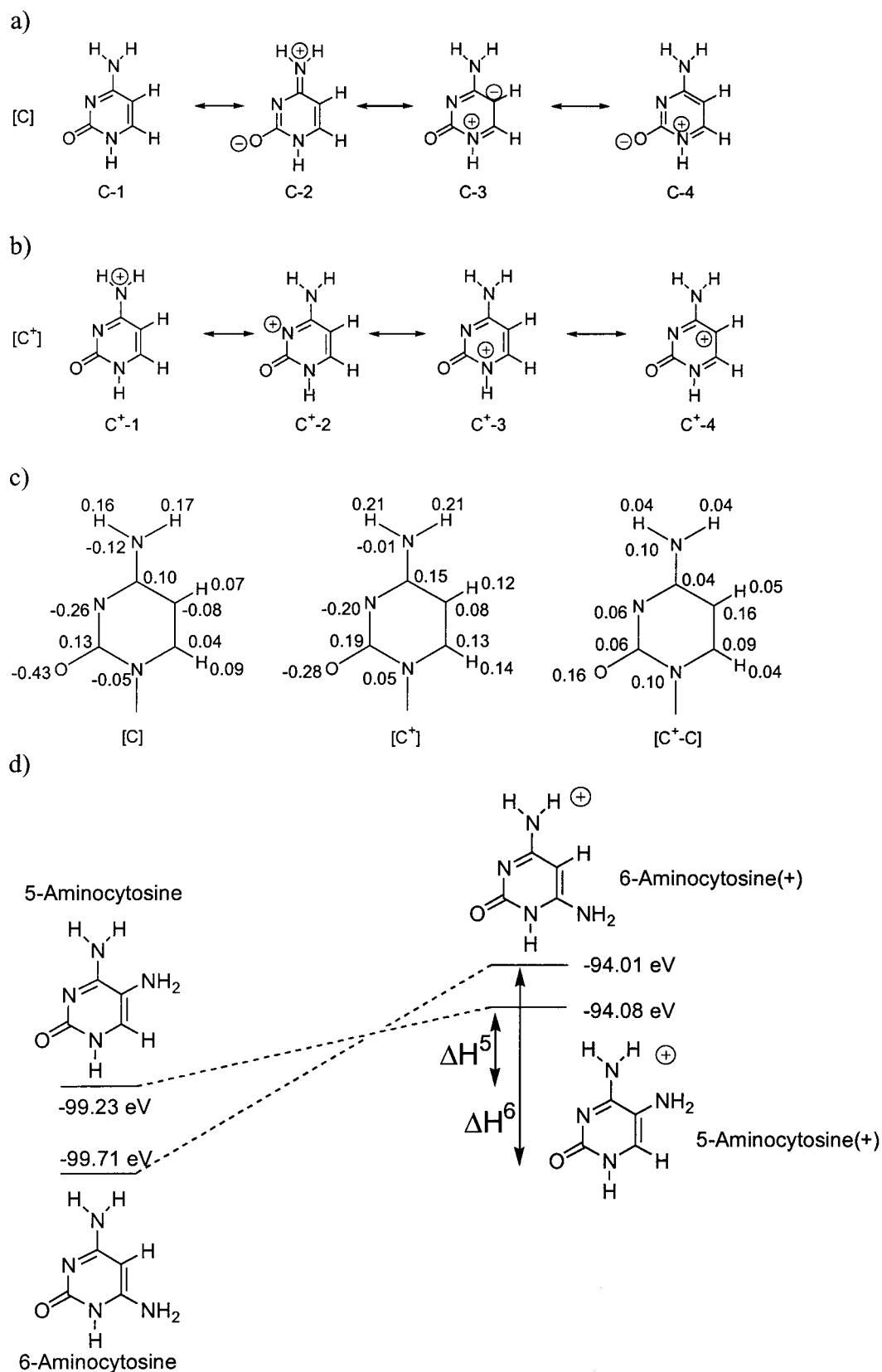
3 and ranges from 0.01 eV for 8-oxoadenine to 0.69 eV for 7-deazaadenine, reflecting the wide range of different observed  $pK_a$  values. For guanine, adenine, and cytosine cationic radicals, experimental estimates of the standard oxidation potential  $E^\circ$  are available and can be compared to the computed  $\Delta G^H$  values. An excellent correlation is observed with the three available experimental standard potentials. For guanine, the total oxidation free energy, including the proton loss, is 6.108 eV, which translates to a standard oxidation potential of 1.67 V. Steenken<sup>36</sup> has deduced an experimental value of 1.58 V. For adenine, 2.14 V is computed, reproducing the experimentally observed value of 2.03 V. The  $E^\circ$  of cytosine has been estimated<sup>36</sup> to be 2.53 V, which is in good agreement with our theoretical value of 2.50 V. The correlation of the calculated and experimentally observed  $pK_a$  values also shows excellent agreement except for thymine, where a deviation of 2.8  $pK_a$  units was obtained. This deviation could not be explained by the existence of more stable structural isomers or different sites of proton abstraction. Only the  $pK_a$  of the most acidic proton for each nucleobase is given in Table 3.

The failure to calculate the shift in potential for 8-oxoadenine is resolved in part if the proton loss step is included. The  $pK_a$  of the 8-oxoadenine radical cation is very high (9.96), which means that the deprotonation correction to the purely electrochemical oxidation potential is small. According to our calculation, the overall  $E^\circ$  of 8-oxoadenine is 5.831 eV, which is essentially identical to the purely electrochemical potential of 5.817 eV listed in Table 2. Since the deprotonation energy correction for the other nucleobases is significant, the disagreement of the oxidation potential ordering noted above is not present in the values corrected for the proton loss. The calculated  $E^\circ$  for 8-oxoadenine is 0.277 eV lower than that of guanine, which is in good agreement with the experiments.

## Discussion

The orbital energy of the HOMO is a good indicator of the oxidation potential, especially for comparisons among a similar series of compounds where the structural and electronic relaxation upon removal of the highest-lying electron are similar. Figure 2 shows three-dimensional plots of the HOMOs of all four natural nucleobases, which are all  $\pi$  orbitals extending over the whole ring system. Tuning the oxidation potential is intrinsically connected to tuning the energy of the HOMO, and rational explanations for shifts in the oxidation potential are available from studying the effects of structural variations on the energy of the HOMO.

## SCHEME 1



Having developed a theoretical model that accurately predicts the trends in redox potentials for the modified nucleobases, we sought to use the model and the associated HOMO energies to gain insight into the chemical nature of the shifts in redox potential. In the case of the aminocytosine derivatives, we were particularly interested in the magnitude of the shift for the

5-amino derivative. While we expected the donating amino group to lower the redox potential, the observed and predicted shift of nearly 1 V was surprising. We therefore sought to use the theoretical model to provide insight into both the magnitude of the shift and the difference in the 5- and 6-amino derivatives.

Parts a and b of Scheme 1 show resonance structures of the

neutral and cationic cytosine molecules, respectively. Of note are structures in the neutral form where the carbon at the 5-position is negatively charged (structure C-3) and in the cationic form where the carbon at the 5-position is positively charged (structure C<sup>+</sup>-4). In contrast, formal charges cannot be assigned to the carbon at the 6-position. These simple considerations predict a larger effect for the 5-amino form. In Scheme 1c, these effects can be considered more quantitatively in the theoretical model by considering the Hirshfeld charges<sup>71</sup> computed for the neutral and cationic forms of cytosine as well as the difference in charges at each atom, [C<sup>+</sup> - C]. Note that this differential charge is commonly known as the Fukui(-) function<sup>72,73</sup> and is the most natural tool for monitoring the response of a molecule undergoing a redox process. As expected, the DFT calculations show that upon oxidation the charge of the carbon at the 5-position changes from -0.08 to 0.08, and a change from 0.04 to 0.13 occurs for the carbon at the 6-position. Scheme 1d gives a sketch of the relative energy profiles for 5- and 6-aminocytosine and shows that although the neutral 6-aminocytosine is energetically more stable than the 5-amino analogue, the dissipation of the positive charge upon oxidation favors the 5-aminocytosine(+) over the 6-aminocytosine(+). The net result is a very small energy difference between the neutral and cationic forms of 5-aminocytosine ( $\Delta H^5$  in Scheme 1d) compared to the large change for 6-aminocytosine ( $\Delta H^6$  in Scheme 1d), giving rise to a very low adiabatic oxidation potential.

## Conclusions

We have used computational methods to identify readily oxidizable derivatives of guanine (8-oxoguanine and 7-deaza-guanine), adenine (8-oxoadenine and 7-deazaadenine), cytosine (5-aminocytosine and 6-aminocytosine), and thymine (5-aminouracil) and have confirmed experimentally that these substituted nucleobases exhibit redox potentials similar to or lower than that of native guanine. On the basis of the computational results, intuitive rationales have been derived that quantitatively examine the effects of different functional groups. None of these derivatives is substituted at the atoms responsible for base pairing, which should allow for development of nucleosides that form native Watson-Crick base pairs and undergo DNA hybridization. This information should enable new diagnostic assays, such as mismatch scoring,<sup>50,53</sup> based on the redox activity of individual nucleotides and new kinds of devices based on electronic coupling in DNA.<sup>74,75</sup>

**Acknowledgment.** This work was supported by the National Science Foundation and Xantho, Inc. J.S.S. thanks the Lineberger Comprehensive Cancer Center for a postdoctoral fellowship, and V.A.S. thanks the National Institutes of Health and the Lineberger Comprehensive Cancer Center. We gratefully acknowledge the North Carolina Supercomputing Center for providing computational time and technical assistance.

**Supporting Information Available:** Coordinates of all optimized structures and electrochemical results for 7-deaza-guanine, 7-deazaadenine, 8-oxoadenine, and 6-aminocytidine. This material is available free of charge via the Internet at <http://pubs.acs.org>.

## References and Notes

- (1) Porath, D.; Bezryadin, A.; de Vries, S.; Dekker, C. *Nature* **2000**, *403*, 635–638.
- (2) Okahata, Y.; Kobayashi, T.; Tanaka, K.; Shimomura, M. *J. Am. Chem. Soc.* **1998**, *120*, 6165–6166.
- (3) Fink, H. W.; Schonenberger, C. *Nature* **1999**, *398*, 407–410.
- (4) Thorp, H. H. *Trends Biotechnol.* **1998**, *16*, 117–121.
- (5) Wang, J.; Bollo, S.; Paz, J. L. L.; Sahlin, E.; Mukherjee, B. *Anal. Chem.* **1999**, *71*, 1910–1913.
- (6) Armistead, P. M.; Thorp, H. H. *Anal. Chem.* **2000**, *72*, 3764–3770.
- (7) Kelley, S. O.; Jackson, N. M.; Hill, M. G.; Barton, J. K. *Angew. Chem., Int. Ed.* **1999**, *38*, 941–945.
- (8) Meggers, E.; Michel-Beyerle, M. E.; Giese, B. *J. Am. Chem. Soc.* **1998**, *120*, 12950–12955.
- (9) Henderson, P. T.; Jones, D.; Hampikian, G.; Kan, Y.; Schuster, G. B. *Proc. Natl. Acad. Sci. U.S.A.* **1999**, *96*, 8353–8358.
- (10) Wan, C.; Fiebig, T.; Schiemann, O.; Barton, J. K.; Zewail, A. H. *Proc. Natl. Acad. Sci. U.S.A.* **2000**, *97*, 14052–14055.
- (11) Burrows, C. J.; Muller, J. G. *Chem. Rev.* **1998**, *98*, 1109–1152.
- (12) Hall, D. B.; Holmlin, R. E.; Barton, J. K. *Nature* **1996**, *382*, 731–735.
- (13) Lewis, F. D.; Liu, X.; Liu, J.; Miller, S. E.; Hayes, R. T.; Wasielewski, M. R. *Nature* **2000**, *406*, 51–53.
- (14) Jortner, J.; Bixon, M.; Langenbacher, T.; Michel-Beyerle, M. E. *Proc. Natl. Acad. Sci. U.S.A.* **1998**, *95*, 12759–12765.
- (15) Schuster, G. B. *Acc. Chem. Res.* **2000**, *33*, 253–260.
- (16) Parr, R. G.; Yang, W. *Density Functional Theory of Atoms and Molecules*; Oxford University Press: New York, 1989.
- (17) Ziegler, T. *Chem. Rev.* **1991**, *91*, 651–667.
- (18) Klamt, A.; Schuurmann, G. *J. Chem. Soc., Perkin Trans.* **1993**, 799–805.
- (19) Pye, C. C.; Ziegler, T. *Theor. Chim. Acta* **1999**, *101*, 396–408.
- (20) Boesch, S. E.; Grafton, A. K.; Wheeler, R. A. *J. Phys. Chem.* **1996**, *100*, 10083–10087.
- (21) Kettle, L. J.; Bates, S. P.; Mount, A. R. *Phys. Chem. Chem. Phys.* **2000**, *2*, 195–201.
- (22) Konecny, R.; Li, J.; Fisher, C. L.; Dillet, V.; Bashford, D.; Noodleman, L. *Inorg. Chem.* **1999**, *38*, 940–950.
- (23) Li, J.; Fisher, C. L.; Chen, J. L.; Bashford, D.; Noodleman, L. *Inorg. Chem.* **1996**, *35*, 4694–4702.
- (24) Li, J.; Nelson, M. R.; Peng, C. Y.; Bashford, D.; Noodleman, L. *J. Phys. Chem. A* **1998**, *102*, 6311–6324.
- (25) Macgregor, S. A.; Moock, K. H. *Inorg. Chem.* **1998**, *37*, 3284–3292.
- (26) Baik, M.-H.; Ziegler, T.; Schauer, C. K. *J. Am. Chem. Soc.* **2000**, *122*, 9143–9154.
- (27) Moock, K. H.; Macgregor, S. A.; Heath, G. A.; Derrick, S.; Boere, R. T. *J. Chem. Soc., Dalton Trans.* **1996**, 2067–2076.
- (28) Mouesca, J.-M.; Chen, J. L.; Noodleman, L.; Bashford, D.; Case, D. A. *J. Am. Chem. Soc.* **1994**, *116*, 11898–11914.
- (29) Raymond, K. S.; Grafton, A. K.; Wheeler, R. A. *J. Phys. Chem. B* **1997**, *101*, 623–631.
- (30) Reynolds, C. A. *Int. J. Quantum Chem.* **1995**, *56*, 677–687.
- (31) Wheeler, R. A. *J. Am. Chem. Soc.* **1994**, *116*, 11048–11051.
- (32) Winget, P.; Weber, E. J.; Cramer, C. J.; Truhlar, D. G. *Phys. Chem. Chem. Phys.* **2000**, *2*, 1231–1239.
- (33) DiLabio, G. A.; Pratt, D. A.; LoFaro, A. D.; Wright, J. S. *J. Phys. Chem. A* **1999**, *103*, 1653–1661.
- (34) Prat, F.; Houk, K. N.; Foote, C. S. *J. Am. Chem. Soc.* **1998**, *120*, 845–846.
- (35) Sugiyama, H.; Saito, I. *J. Am. Chem. Soc.* **1996**, *118*, 7063–7068.
- (36) Steenken, S.; Jovanovic, S. V. *J. Am. Chem. Soc.* **1997**, *119*, 617–618.
- (37) Steenken, S. *Biol. Chem.* **1997**, *378*, 1293–1297.
- (38) Steenken, S.; Jovanovic, S. V.; Bietti, M.; Bernhard, K. *J. Am. Chem. Soc.* **2000**, *122*, 2373–2374.
- (39) Shafirovich, V.; Dourandin, A.; Luneva, N. P.; Geacintov, N. E. *J. Phys. Chem. B* **2000**, *104*, 137–139.
- (40) Weatherly, S. C.; Yang, I. V.; Thorp, H. H. *J. Am. Chem. Soc.* **2001**, *123*, 1236–1237.
- (41) Bard, A. J.; Faulkner, L. R. *Electrochemical Methods*; John Wiley and Sons: New York, 1980.
- (42) Steenken, S. *Chem. Rev.* **1989**, *89*, 503–520.
- (43) Steenken, S.; Telo, J. P.; Novais, H. M.; Candeias, L. P. *J. Am. Chem. Soc.* **1992**, *114*, 4701–4709.
- (44) Yanagawa, H.; Ogawa, Y.; Ueno, M. *J. Biol. Chem.* **1992**, *267*, 13320–13326.
- (45) Baerends, E. J.; Bérces, A.; Bo, C.; Boerrigter, P. M.; Cavallo, L.; Deng, L.; Dickson, R. M.; Ellis, D. E.; Fan, L.; Fischer, T. H.; Fonseca Guerra, C.; van Gisbergen, S. J. A.; Groeneveld, J. A.; Gritsenko, O. V.; Harris, F. E.; van den Hoek, P.; Jacobsen, H.; van Kessel, G.; Kootstra, F.; van Lenthe, E.; Osinga, V. P.; Philipsen, P. H. T.; Post, D.; Pye, C. C.; Ravenek, W.; Ros, P.; Schipper, P. R. T.; Schreckenbach, G.; Snijders, J. G.; Sola, M.; Swerhone, D.; te Velde, G.; Vermooijs, P.; Versluis, L.; Visser, O.; van Wezenbeek, E.; Wiesenekker, G.; Wolff, S. K.; Woo, T. K.; Ziegler, T.; Fonseca Guerra, C.; Snijders, J. G.; te Velde, G.; Baerends, E. J. *Theor. Chem. Acc.* **1998**, *99*, 391–403.

- (46) Vosko, S. H.; Wilk, L.; Nusair, M. *Can. J. Phys.* **1980**, *58*, 1200–1211.
- (47) Perdew, J. P.; Wang, Y. *Phys. Rev. B* **1992**, *45*, 13244.
- (48) Goldman, D.; Kalman, T. I. *Nucleosides Nucleotides* **1983**, *2*, 175–187.
- (49) Friedland, M.; Visser, D. W. *Biochim. Biophys. Acta* **1961**, *51*, 148–152.
- (50) Johnston, D. H.; Glasgow, K. C.; Thorp, H. H. *J. Am. Chem. Soc.* **1995**, *117*, 8933–8938.
- (51) Johnston, D. H.; Welch, T. W.; Thorp, H. H. *Metal Ions Biol. Syst.* **1996**, *33*, 297–324.
- (52) Johnston, D. H.; Thorp, H. H. *J. Phys. Chem.* **1996**, *100*, 13837–13843.
- (53) Ropp, P. A.; Thorp, H. H. *Chem. Biol.* **1999**, *6*, 599–605.
- (54) Yang, I. V.; Thorp, H. H. *Inorg. Chem.* **2001**, *40*, 1690–1697.
- (55) Hickerson, R. P.; Prat, F.; Muller, J. G.; Foote, C. S.; Burrows, C. *J. Am. Chem. Soc.* **1999**, *121*, 9423–9428.
- (56) Kelley, S. O.; Barton, J. K. *Science* **1999**, *283*, 375–381.
- (57) Throughout this paper, we refer to the complex with the lowest potential that would oxidize the particular nucleobase to give detectable current enhancements. A particular nucleobase will also react with complexes of higher potential and not with complexes of lower potential. For example, 8-oxoadenine reacts with  $\text{Ru}(\text{bpy})_3^{3+}$  and  $\text{Fe}(\text{bpy})_3^{3+}$ , but not with  $\text{Os}(\text{bpy})_3^{3+}$ .
- (58) Guerra, C. F.; Bickelhaupt, F. M.; Snijders, J. G.; Baerends, E. J. *J. Am. Chem. Soc.* **2000**, *122*, 4117–4128.
- (59) Guerra, C. F.; Bickelhaupt, F. M.; Snijders, J. G.; Baerends, E. J. *Chem.-Eur. J.* **1999**, *5*, 3581–3594.
- (60) Guerra, C. F.; Bickelhaupt, F. M. *Angew. Chem., Int. Ed.* **1999**, *38*, 2942–2945.
- (61) Gorb, L.; Leszczynski, J. *J. Am. Chem. Soc.* **1998**, *120*, 5024–5032.
- (62) Gu, J.; Leszczynski, J. *J. Phys. Chem. A* **1999**, *103*, 577–584.
- (63) Zhanpeisov, N. U.; Cox, W. W., Jr.; Leszczynski, J. *J. Phys. Chem. A* **1999**, *103*, 4564–4571.
- (64) For a simple oxidation process  $\text{B} \rightarrow \text{B}^+ + \text{e}^-$  (B = nucleobase), the energy difference, including the continuum solvation model in the electronic structure calculation, is the adiabatic redox potential that is commonly measured using electrochemical techniques, such as cyclic voltammetry (CV). Usually, solution redox potentials are reported as relative potentials; that is, they are referenced to a standard electrode with a specific potential. For the standard hydrogen electrode (SHE), the absolute potential has been determined experimentally to be 4.43 eV (Reiss, H.; Heller, A. *J. Phys. Chem.* **1985**, *89*, 4207–4213). So, to relate experimental redox potentials to the computed absolute energies, the reference potential needs to be added.
- (65) Orlov, V. M.; Smirnov, A. N.; Varshavsky, Y. M. *Tetrahedron Lett.* **1976**, 4377–4378.
- (66) Lyne, P. D.; Karplus, M. *J. Am. Chem. Soc.* **2000**, *122*, 166–167.
- (67) Richardson, W. H.; Peng, C.; Bashford, D.; Noodleman, L.; Case, D. A. *Int. J. Quantum Chem.* **1997**, *61*, 207–217.
- (68) Li, J.; Fisher, C. L.; Konecny, R.; Bashford, D.; Noodleman, L. *Inorg. Chem.* **1999**, *38*, 929–939.
- (69) Chen, J. L.; Noodleman, L.; Case, D. A.; Bashford, D. *J. Phys. Chem.* **1994**, *98*, 11059–11068.
- (70) Tawa, G. J.; Topol, I. A.; Burt, S. K.; Caldwell, R. A.; Rashin, A. A. *J. Chem. Phys.* **1998**, *109*, 4852–4863.
- (71) Hirshfeld, F. L. *Theor. Chim. Acta B* **1977**, *44*, 129–138.
- (72) Fukui, K.; Yonezawa, T.; Shingu, H. *J. Chem. Phys.* **1952**, *20*, 722–725.
- (73) Fukui, K. *Science* **1982**, *218*, 747–754.
- (74) Leone, A. M.; Weatherly, S. C.; Williams, M. E.; Thorp, H. H.; Murray, R. W. *J. Am. Chem. Soc.* **2001**, *123*, 218–222.
- (75) Mirkin, C. A.; Taton, T. A. *Nature* **2000**, *405*, 626–627.